Faithful replication of grating patterns in polymer through electrohydrodynamic instabilities

2014 J. Micromech. Microeng. 24 075006

(http://iopscience.iop.org/0960-1317/24/7/075006)

IOP Publishing Journal of Micromechanics and Microengineering
J. Micromech. Microeng. **24** (2014) 075006 (9pp) doi:10.1088/0960-1317/24/7/075006

Faithful replication of grating patterns in polymer through electrohydrodynamic instabilities

H Li[1,2], W Yu[1], T Wang[1], H Zhang[1], Y Cao[1], E Abraham[3] and M P Y Desmulliez[3]

[1] State Key Laboratory of Applied Optics, Changchun Institute of Optics, Fine Mechanics & Physics, Chinese Academy of Sciences, No.3888, Dongnanhu Road, Changchun, Jilin, People's Republic of China
[2] University of Chinese Academy of Sciences, Beijing, 10039, People's Republic of China
[3] MIcroSystems Engineering Centre (MISEC), School of Engineering & Physical Sciences, Heriot-Watt University, Edinburgh EH14 4AS, UK

E-mail: yuwx@ciomp.ac.cn and m.desmulliez@hw.ac.uk

Received 9 March 2014, revised 20 April 2014
Accepted for publication 6 May 2014
Published 29 May 2014

Abstract

Electrohydrodynamic instability patterning (EHDIP) as an alternative patterning method has attracted a great deal of attention over the past decade. This article demonstrates the faithful transfer of patterns with a high aspect ratio onto a polymer film via electrohydrodynamic instabilities for a given patterned grating mask. We perform a simple mathematical analysis to determine the influence of process parameters on the pressure difference ΔP. Through numerical simulation, it is demonstrated that thick films subject to large electric fields are essential to realize this faithful replication. In particular, the influence of the material properties of the polymer on pattern replication is discussed in detail. It is found that, to achieve the smaller periodic patterns with a higher resolution, film with a larger value of the dielectric constant and smaller value of the surface tension should be chosen. In addition, an ideal replication of the mask pattern with a short evolution time is possible by reducing the viscosity of the polymer liquid. Finally, the experiments of the pattern replication with and without defects are demonstrated to compare with the numerical simulation results. It is found that experiments are in good agreement with the simulation results and prove that the numerical simulation method provides an effective way to predict faithful replication.

Keywords: faithful replication, electrohydrodynamic instabilities, grating patterns

(Some figures may appear in colour only in the online journal)

1. Introduction

Recently, electrohydrodynamic instability as a new technique for patterning thin polymer films has attracted a great deal of attention [1, 2]. The advantage of this patterning technique is that the pattern can be formed through a one-step process with inexpensive equipment in comparison with traditional photolithographic methods. In this patterning technique, a thin polymer film deforms and self-assembles into micro and nanostructures under either a featureless mask or patterned mask subject to a high electrostatic voltage. The successful replication of sub-micron periodic grating structures in polymer has been demonstrated by this method [3, 4].

Figure 1 shows the experimental setup used in this patterning technique. A polymer film deposited on a substrate is heated above its glass transition temperature and then annealed for a period of time in the presence of an electrostatic field spatially modulated by a patterned mask. Under such a field configuration, the rheological behavior of the liquid membrane can lead to an ideal replica of the pattern present on the upper electrode. Upon cooling the system back to the room temperature, solidified micro/nanostructures

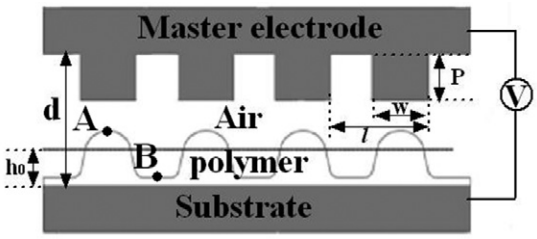

Figure 1. Schematic diagram of the thin film resting on a rigid substrate subjected to an externally heterogeneous electric field.

can be obtained. Such an integration of the top-down and bottom-up methods has potential applications in the fabrications of micro-electro-mechanical systems, chemical or biological sensors, optoelectronic devices, etc.

Numerous theoretical and experimental works have been carried out to understand this phenomenon [5–24]. These studies are mainly based on linear stability analysis, whereas the dynamic evolution process of the interface growth can be studied by nonlinear simulation. A lot of simulations demonstrate that, under a featureless mask, the polymer film organizes itself into hexagonal arrays, which is in agreement with weakly nonlinear analysis [25–32]. The order of the final hexagonal pattern largely depends on the thickness ratio ξ of the air gap to the film thickness. Under patterned masks however, well-ordered polymeric microstructures can be obtained over large areas, which means the pattern of a mask can be replicated in the film.

Full numerical simulations also can explain the dynamic behavior of the EHDIP process and provide insights on intelligent design of masks to produce long range ordered patterns. Kim's simulations reveal the rich dynamics and show that the final structure is not solely determined by energetics: the kinetic process can play an important role. Tuning the electric field can produce a variety of patterns [25]. Verma gave the conditions for ideal templating of the top electrode pattern for a continuous sinusoidal profile in the film [26]. In a previous work, we have reported how to define the limit period, LP, i.e. the fabrication limit of the periodic nanostructures by employing finite element analysis methods [33]. Tian gave a generalized formulation for the numerical characterization of the EHDP processes by coupling liquid dielectrophoresis (L-DEP) and the phase field of the air–liquid dual phase. It has also been found that the scale effects such as the liquid–solid interface slip, L-DEP wetting angle, and non-Newtonian viscosity of the polymer can impact the accuracy of the numerical simulation performed at micro or nanoscale tremendously [34]. However, one practical issue is how one can guarantee the faithful replication of the pattern in the mask electrode into the polymer film for a given mask with grating patterns. In other words, how to find the critical conditions under which one can achieve optimum replication of the mask in polymer, which is not answered by previous simulation works. This article is dedicated to answering this question by using the finite difference method to solve the partial differential equation of the dynamic evolution of the air–film interface, and to find the critical conditions under which faithful replication can be achieved for high aspect ratio in polymer for a given mask. A central difference scheme with the Everett method interpolation was used for spatial discretization of the equation. The time integration was done using Gear's method, which is especially suitable for stiff equations [26]. The influence of process parameters on the pressure difference ΔP was first studied with the help of a simple mathematical analysis. Furthermore, how the material parameters of the film such as dielectric constant and surface tension affect the period of the mask in the replication process was studied. The evolution time of the EHDIP process is also discussed. Finally, experimental validation of the numerical simulation is demonstrated through manufacturing perfect and defective replicas of the mask.

2. Theoretical analysis

A thin polymer film under the influence of the homogeneous electric field, which is considered to be an incompressible Newtonian and perfect dielectric medium, is spun-coated on a rigid solid substrate with high surface energy. We ignore inertial effects in both fluids, so the governing equations for motion are the following continuity and Navier–Stokes equations:

$$\nabla \cdot \mathrm{v}_i = 0 \cdot \tag{1}$$

$$-\nabla p_i + \mu_i \nabla^2 \mathrm{v}_i = 0 \cdot \tag{2}$$

where V_i is the velocity vector in fluid i (i =1 for the film and 2 for the bounding fluid), p_i is the pressure in fluid i, and μ_i is the viscosity of fluid i. The fluid velocities satisfy no-slip and no-penetration conditions at the bottom and upper plates and therefore,

$$\mathrm{v}_1 = 0 \text{ at } z = 0 \quad \mathrm{v}_2 = 0 \text{ at } z = d \tag{3}$$

At the interface y=h(x) between two fluids, the system satisfies continuity of velocity conditions and then we have,

$$(\mathrm{v} \cdot \mathrm{n})_1 = (\mathrm{v} \cdot \mathrm{n})_2 . \tag{4}$$

The kinematic condition at the interface describes the evolution of the interface position h(x, t). Because there is no mass transfer at the interface, the normal velocity of V is equal to the normal velocity at the interface h(x, t),

$$\mathrm{v}_1(y = h(x)) = \mathrm{v}_2(y = h(x)) = \frac{\partial h}{\partial t} + \mathrm{v} \cdot \nabla_s h . \tag{5}$$

Because the lateral length scale is much larger than the film thickness, lubrication approximation theory or long scale approximation is generally used to simplify the N-S equation. By using the kinematic boundary, the nonlinear evolution equation of the interface can be obtained [26, 28, 36]:

$$3\mu(\partial h / \partial t) - \nabla \cdot [h^3 \nabla P] = 0. \tag{6}$$

Later, we perform a simple mathematical analysis that is sufficiently realistic to capture the essential physics of the EHDIP process with the aim of determining the influence of process parameters on the pressure difference ΔP between the peak A and valley B shown in figure 1. Since the large value of pressure difference ΔP can ensure a faithful replication

of the pattern onto polymer film [35]. Here a 'faithful replication' means that polymer film replicates the gratings on mask exactly. This is of practical importance because those polymeric gratings with high aspect ratio are desirable to facilitate etching and other pattern transfer processes. For the homogeneous electric field, the total pressure at the interface in the long wavelength limit is denoted by:

$$p = p_0 - \gamma \frac{\partial^2 h}{\partial x^2} + p_{el}(h) + p_{\mathrm{dis}}(h) \tag{7}$$

where P_0 denotes atmospheric pressure and γ is the surface tension. The second term, the Laplace pressure, plays an important role in maintaining the stability of the film. The third term, electrostatic pressure, in terms of mathematic equation, can be described by:

$$p_{el} = -\varepsilon_0 \varepsilon_r (\varepsilon_r - 1) E_p^2 \tag{8}$$

$$E_p = \frac{U}{\varepsilon_r d - (\varepsilon_r - 1)h} \tag{9}$$

where E_p is the electric field strength in the polymer film, ε_0 is the dielectric permittivity of the vacum, ε_r is the relative dielectric constant of the polymer film, U is the applied voltage, d is the separation distance between the template and the substrate, h is the film thickness. The fourth term denotes the disjoining pressure.

Under the heterogeneous electric field, assuming the interface profile is described by $h=h_0+\xi\cos(kx)$, then the pressure at the peak A and valley B on the interface (in figure 1) would be (referring to equation (7[37]))

$$P_A = P_0 - \frac{V^2 \varepsilon_0 (\varepsilon_r - 1)\varepsilon_r}{2[h_0 + \xi + (d - p - h_0 - \xi)\varepsilon_r]^2} + \gamma \xi k^2 \tag{10}$$

$$P_B = P_0 - \frac{V^2 \varepsilon_0 (\varepsilon_r - 1)\varepsilon_r}{2[h_0 - \xi + (d - h_0 + \xi)\varepsilon_r]^2} - \gamma \xi k^2 \tag{11}$$

The pressure difference ΔP between point A and B would be

$$\Delta P = P_B - P_A = -2\gamma \xi k^2 + \frac{V^2 \varepsilon_0 (\varepsilon_r - 1)\varepsilon_r}{2} \left[\frac{1}{[h_0 + \xi + (d - p - h_0 - \xi)\varepsilon_r]^2} - \frac{1}{[h_0 - \xi + (d - h_0 + \xi)\varepsilon_r]^2} \right] \tag{12}$$

A strong lateral gradient in the pressure possibly induces additional flow and overwhelms the spinodal effects [38], ensuring the perfect transfer of the electrode pattern into the polymer film in the absence of any physical contact between the pattern-directing template and the liquid film. In the following, we will discuss the influence of process parameters such as surface tension on the pressure difference ΔP. The partial derivative of ΔP with respect to γ can be expressed by,

$$\frac{\partial \Delta p}{\partial \gamma} = -2\xi k^2 < 0 \tag{13}$$

Apparently, the partial derivative of ΔP with respect to γ is less than zero. Therefore, decreasing the surface tension is helpful for increasing the pressure difference. The partial derivative of ΔP with respect to initial film thickness h_0 is shown in equation (14)

$$\frac{\partial \Delta p}{\partial h_0} = \frac{V^2 \varepsilon_0 (\varepsilon_r - 1)^2 \varepsilon_r}{4} \left[\frac{1}{[h_0 + \xi + (d - p - h_0 - \xi)\varepsilon_r]^{3/2}} - \frac{1}{[h_0 - \xi + (d - h_0 + \xi)\varepsilon_r]^{3/2}} \right] \tag{14}$$

Because the difference between the two denominators in the brackets on the right-hand side of the equation is less than zero in equation (15) and other coefficients are larger than zero,

$$[h_0 + \xi + (d - p - h_0 - \xi)\varepsilon_r] - [h_0 - \xi + (d - h_0 + \xi)\varepsilon_r] = 2\xi - 2\xi\varepsilon_r - p\varepsilon_r < 0 \tag{15}$$

$$\frac{\partial \Delta P}{\partial h_0} > 0 \tag{16}$$

Hence, the partial derivative of ΔP with respect to h_0 is larger than zero. Therefore, increasing the value of the film thickness is helpful for increasing the pressure difference ΔP.

The partial derivative of ΔP with respect to applied voltage V is shown in equation (17),

$$\frac{\partial \Delta P}{\partial V} = V \varepsilon_0 (\varepsilon_r - 1)\varepsilon_r \left[\frac{1}{[h_0 + \xi + (d - p - h_0 - \xi)\varepsilon_r]^2} - \frac{1}{[h_0 - \xi + (d - h_0 + \xi)\varepsilon_r]^2} \right] \tag{17}$$

Due to equation (15) and the other terms being larger than zero, the partial derivative of ΔP with respect to V is larger than zero,

$$\frac{\partial \Delta P}{\partial V} > 0 \tag{18}$$

Therefore, increasing the value of the applied voltage is helpful for increasing the pressure difference ΔP.

The partial derivative of ΔP with respect to the relative dielectric constant of the polymer film ε_r is shown in equation (19),

$$\frac{\partial \Delta P}{\partial \varepsilon_r} = \frac{V^2 \varepsilon_0}{2} \left\{ \begin{array}{l} (2\varepsilon_r - 1) \left[\dfrac{1}{[h_0 + \xi + (d - p - h_0 - \xi)\varepsilon_r]^2} - \dfrac{1}{[h_0 - \xi + (d - h_0 + \xi)\varepsilon_r]^2} \right] + \\ \dfrac{(\varepsilon_r - 1)\varepsilon_r}{2} \left[\dfrac{d - h_0 + \xi}{[h_0 - \xi + (d - h_0 + \xi)\varepsilon_r]^{3/2}} - \dfrac{d - p - h_0 - \xi}{[h_0 + \xi + (d - p - h_0 - \xi)\varepsilon_r]^{3/2}} \right] \end{array} \right\} \tag{19}$$

Because the equation (15) and the difference between the two denominators in the second brackets (equation (20)) is larger than zero,

$$(d-h_0+\xi)-(d-p-h_0-\xi)=p+2\xi>0 \tag{20}$$

Therefore, the partial derivative of ΔP with respect to ε_r is larger than zero.

$$\frac{\partial \Delta P}{\partial \varepsilon_r}>0 \tag{21}$$

Therefore, increasing the value of relative dielectric constant of the polymer film is helpful for increasing the pressure difference ΔP. These results are of paramount importance to the design, optimization and fabrication of nanochannels for practical applications.

3. Presentation of the simulation model

In the model, the polymer film is considered to be an isothermal and perfect dielectric fluid confined between the top patterned mask and the bottom substrate as shown in figure 1. The initial film thickness is represented by h_0. When the film is perturbed by an externally heterogeneous electrostatic field, the local film is destabilized, forming the replica of the mask in one-step. The mask with voltage V is positioned above the substrate at a distance d. For a patterned mask, the depth of electrode protrusions, the width of the electrode protrusion, the period, are denoted by p, w, and l, respectively, as shown in figure 1. The three-dimensional model provides a comprehensive computational study of the dynamic self-assembly process. The finite difference method is used to solve the partial differential equation of the dynamic evolution of the air-film interface [26, 28]. We converted the partial differential equations of the dynamic evolution of the air-film interface to an ordinary differential equation using a finite difference discretisation with respect to space. The resulting equation is then integrated with respect to time by the stiff Gear method [40]. Periodic boundary conditions were applied at the domain boundaries, and the initial condition was a volume preserving random disturbance of small amplitude. Numerical accuracy and convergence were checked by varying the number of grid points. The electric field can be obtained by solving the analytical equation (9). A van der Waals-like repulsive force is imposed on the top electrode and substrate to prevent the air-film interface from penetrating the upper electrode. The form of the repulsive force is similar to that used in reference [26].

4. Simulation results and discussions

Representative results are presented in this section. Unless otherwise noted, the following material parameters are used in our simulations. The viscosity μ of the film is 1 Pa.s, the surface tension γ is 0.038 J m^{-2}, dielectric constant of the film ε_1 is 2.5 and permittivity of free space is 8.85×10^{-12} CV^{-1} m^{-1}, the applied voltage between two electrodes is 100 V, the separation between two electrodes is 1 μm. For convenient observation of the self-assembly process of the film, six successive pictures taken over time are given, and then six 3 D surface profiles of the images corresponding to the former six pictures are shown.

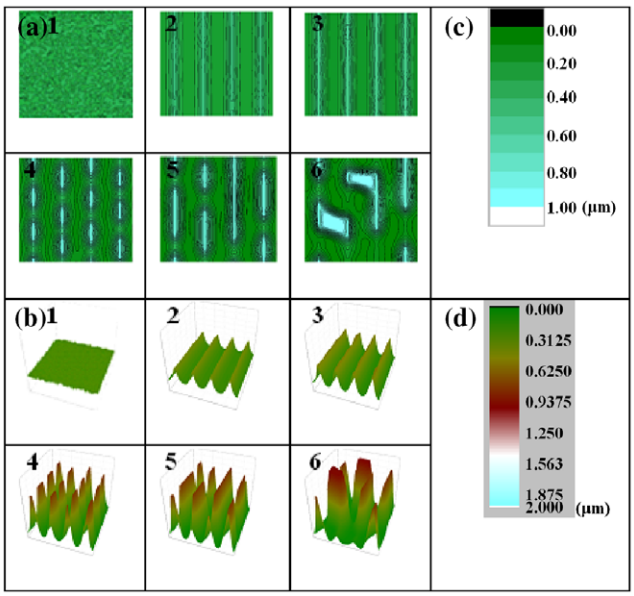

Figure 2. (*a*) Evolution of a 0.30 μm thick film in the presence of a periodically varying electric field in a 14.8 μm×14.8 μm domain. The top electrode pattern consists of four periodically gratings with a length of 14.8 μm, a width of 0.2 μm and a height of 0.2 μm. The dimensionless time of evolution for images 1–6 are T =0, 6268, 10745, 22385, 39398 and 125360 respectively. (*b*) 3 D surface profiles of the images obtained in part (*a*).

On the basis of intensive simulations, it is found that the final morphology of the film in the presence of a spatially modulated periodic electric field crucially depends on the periodicity of the top electrode pattern, the surface tension and dielectric constant of the film. However, regardless of the above-mentioned conditions, the initial structure always organizes itself on a length scale close to the pattern periodicity l. However, later stages of evolution are dominated by l, together with the surface tension and dielectric constant of the film. By tuning the material property of the film, initial film thickness and the applied voltage, one should be able to obtain the ideal replica of the top electrode pattern in the film.

The following section describes the means to obtain the perfect replica of the pattern for the given mask in the polymeric film. The pattern chosen for the mask is a grating of period of 3.7 μm, for a depth and width of the grating stripes of 0.2 μm. Figures 2 and 3 depict the final morphology of the formed structure in the thin film. For different initial film thicknesses h_0, 0.30 μm in figure 2 and 0.33 μm in figure 3, parallel ridges are formed under each protrusion of the top electrode where the electric field is the strongest. If the evolution time is long enough, a secondary instability develops and leads to the transformation of the grating patterns into pillar-like structures with a length scale of natural wavelength λ [5]. In the sixth image of figure 2(*a*), the adjacent pillar-like structures merge with each other both along and perpendicular to the directions of the stripe, therefore preventing the accurate replication of the mask. This incompleteness of the replica shown in figure 2 results from the small pressure difference ΔP, that is to say the effect of varying electric field in the EHDIP process is weak. In general, when the pressure difference ΔP is small, the thin

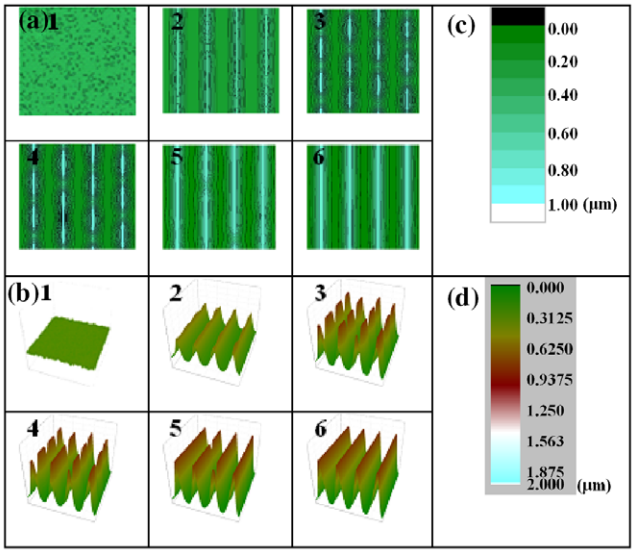

Figure 3. (*a*) Evolution of a 0.33 μm thick film in the presence of a periodically varying electric field in a 14.8 μm × 14.8 μm domain. The top electrode pattern consists of four gratings with a length of 14.8 μm, a width of 0.2 μm and a height of 0.2 μm. The dimensionless time of evolution for images 1–6 are T = 0, 4789, 8745, 8418, 12782 and 17491, respectively. (*b*) 3 D surface profiles of the images obtained in part (*a*).

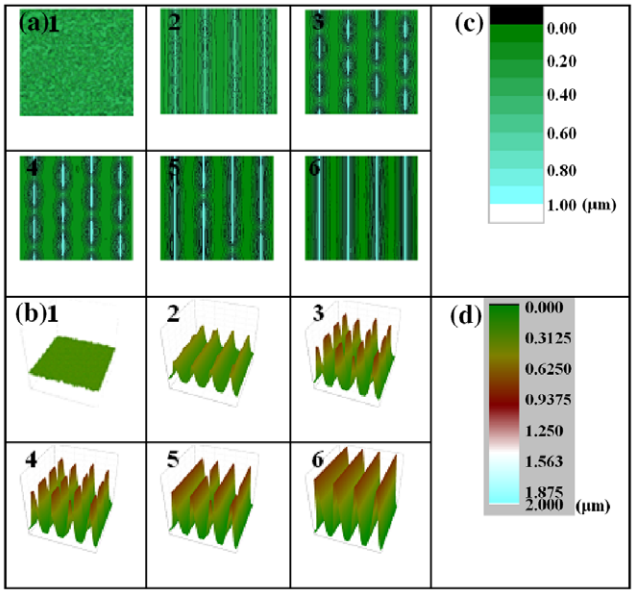

Figure 4. (*a*) Evolution of a 0.30 μm thick film under the same conditions in figure 3 except that the applied voltage is 111 V. The dimensionless time of evolution for stages 1–6 are T = 0, 9515, 16311, 20389, 28545, and 67966, respectively. (*b*) 3 D surface profiles of the images obtained in part (*a*).

film initially grows into sinusoidal waves, which replicate the patterned mask. Those waves then start breaking into individual pillars because of the enormous surface energy penalty for further growth without changing the periodicity. Finally, the intrinsic characteristic length sets in and forms pillars, which is totally different than the gratings pattern on the mask.

In order to realize the replication process, the film thickness has been gradually increased to a critical value of 0.33 μm in order to increase the pressure difference ΔP. A different final morphological feature is obtained and shown in figure 3. The merging of adjacent pillar-like structures occurs this time in the direction of the stripe so that the pattern in the mask can be replicated in the film. In general, by increasing the value of the film thickness, the second instability can be suppressed so that one can achieve a good replication of the pattern in the film.

4.1. Influence of the electrostatic field

In order to realize the replication of the mask in figure 2, we adopt another method by gradually increasing the value of the applied voltage to a critical value with the aim of obtaining the larger pressure difference ΔP. For convenience of comparison, the periodicity l in figure 4 is the same as the value used in figure 2, but the applied voltage is set to be 111 V in order to investigate the effect of electric field strength on the final structures. In the process of increasing the value of the voltage, the order of the feature in the polymer film becomes uniform gradually. The simulation result shows that in this case the pattern on the top electrode can be faithfully replicated in the film. The pillars in line are incorporated into stripes by absorbing the surrounding material at t = 20389.9, so that continuous periodic liquid stripes are formed corresponding to the positions of the trough and crest of the top electrode, resulting in a nearly perfect templating. Thus, the condition for ideal templating can be generalized on the basis of this result. It was indeed verified that an ideal replication of the electrode pattern becomes possible by increasing the strength of the applied electric field if the induced features are non-uniform.

4.2. Influence of the surface tension

The reduction of the surface tension favors smaller features. Decreasing the surface tension means that a larger pressure difference ΔP can be obtained. When applying the same conditions as in figure 2, except for the surface tension being reduced to 0.019 J m^{-2}, the final feature in figure 5 resembles the case when the applied voltage is 111 V. The final pattern has the same periodicity as that of the electrode pattern. A useful result found here is that it is propitious to attain the desired ordered structures in thin film of soft materials by decreasing the surface tension. In this situation, the period l of the mask can be decreased to 2.9 μm so that the replication is still successful. Therefore, by tuning the surface tension of the material, a replica of the mask with a smaller period could be obtained. Figure 6 shows the relationship of the period of the mask, which can be replicated against surface tension γ. In general, when the surface tension becomes smaller, a mask with smaller period l can also be replicated. Specifically, the smallest period that can be achieved is 1.7 μm when electrode protrusion has a width of 0.3 μm and a height of 0.3 μm for an applied voltage of 100 V and surface tension γ of 0.019 J m^{-2}.

4.3. Influence of the dielectric constant

When applying the same conditions as in figure 2 except that the dielectric constant is increased from 2.5 to 4, i.e.

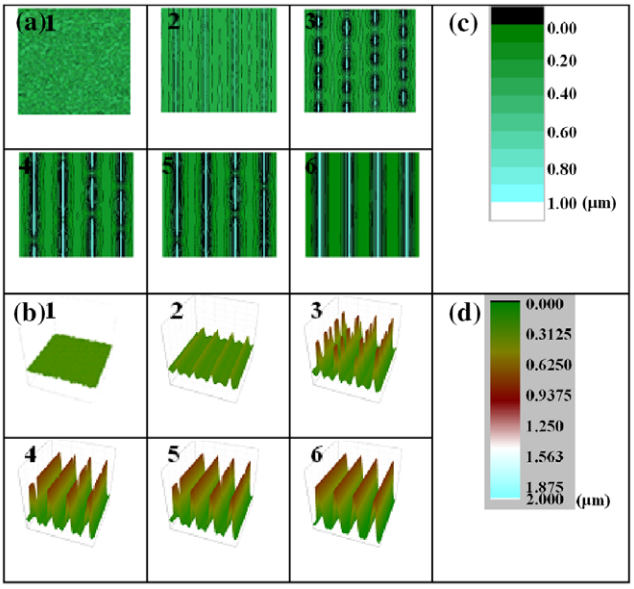

Figure 5. (*a*) Evolution of a 0.30 μm thick film under the same conditions as in figure 3 except the surface tension is 0.019 J m^{-2}. The dimensionless time of evolution for images 1–6 are T =0, 3581, 10745, 23281, 25072 and 71634, respectively. (*b*) 3 D surface profiles of the images in part (*a*).

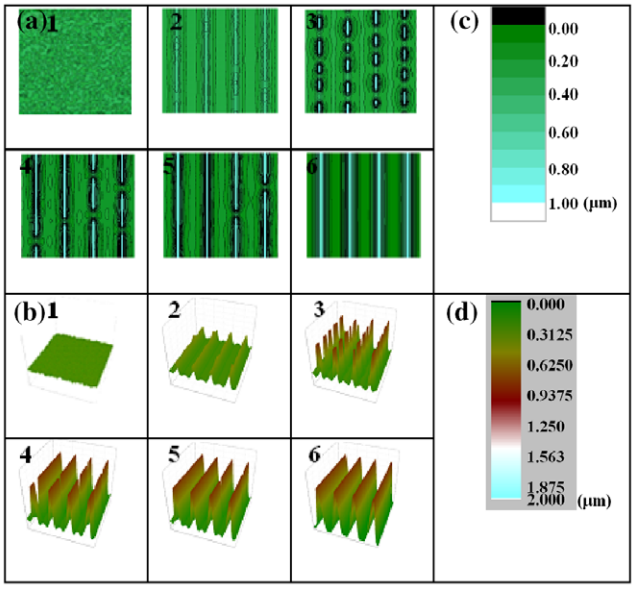

Figure 7. (*a*) Evolution of a 0.30 μm thick film under the same conditions as in Figure 3 with the exception of a dielectric constant of 4. The dimensionless time of evolution for images 1–6 are T = 0, 18338, 27507, 55015, 73353 and 458468, respectively. (*b*) 3 D surface profiles of the images obtained in part (*a*).

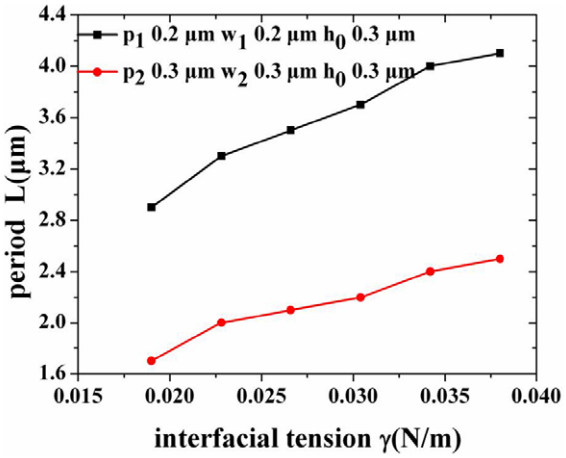

Figure 6. The dependence of the period l on the surface tension γ for the case w=0.2 μm, 0.3 μm, and p=0.2 μm, 0.3 μm, h_0=0.3 μm and d=1 μm.

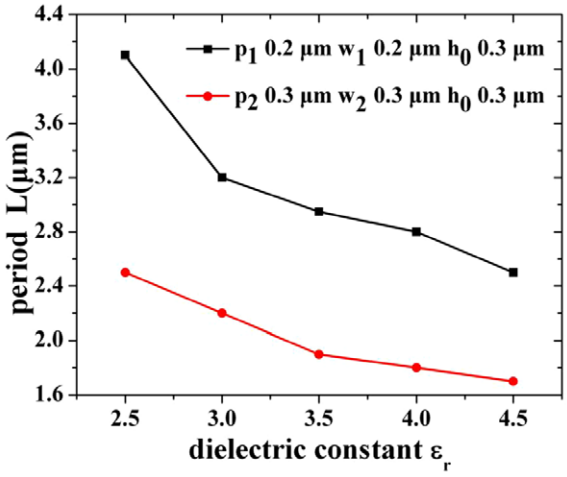

Figure 8. The variation of the period l with the change of the dielectric constant ε for the case of: w = 0.2 μm, 0.3 μm, and p = 0.2 μm, 0.3 μm, ψ = 100 V, h_0 = 0.3 μm and d = 1 μm.

the pressure difference ΔP is increased, it is found that the electrode pattern can be ideally replicated into the film as shown in figure 7. The strength of the spatially modulated electric field is indeed enhanced so that it overcomes the natural characteristic wavelength based on average separation between two electrodes. In this situation, the mask with a period of 2.8 μm can be replicated. In general, increasing the electrostatic stress at the interface by enhancing the dielectric contrast between bottom and top layers allows the replication of smaller features. Figure 8 shows the relationship of the period of the mask, which can be replicated against dielectric constant ε. As shown, l decreases when the dielectric constant increases. Specifically, the smallest period can be achieved here is 1.7 μm for electrode protrusions with a width of 0.3 μm and a height of 0.3 μm when a voltage 100 V is applied and the dielectric constant is 4.5.

4.4. Influence of the viscosity

Depending on the viscosity of the polymer film, the duration for pattern formation varies drastically from seconds to weeks. Figure 9 shows the effect of the viscosity of the film on the final morphological feature in the film. In this case, the viscosity of the film is 0.1 Pa.s. The result shows that by decreasing the viscosity of the film, the replication process cannot be improved effectively. But the evolution time of the dynamic process under the heterogeneous field is reduced significantly. In order to compare the time of evolution for different viscosities of the

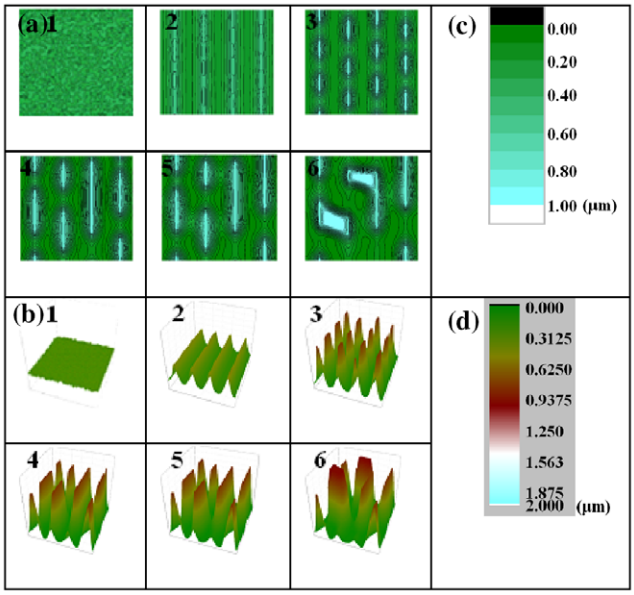

Figure 9. (*a*) Evolution of a 0.30 μm thick film under the same condition in figure 3 except the viscosity of the film is 0.1 Pa.s. The dimensionless time of evolution for images 1–6 are T = 0, 8954, 17908, 71634, 89542 and 125368, respectively. (*b*) 3 D surface profiles of the images obtained in part (*a*).

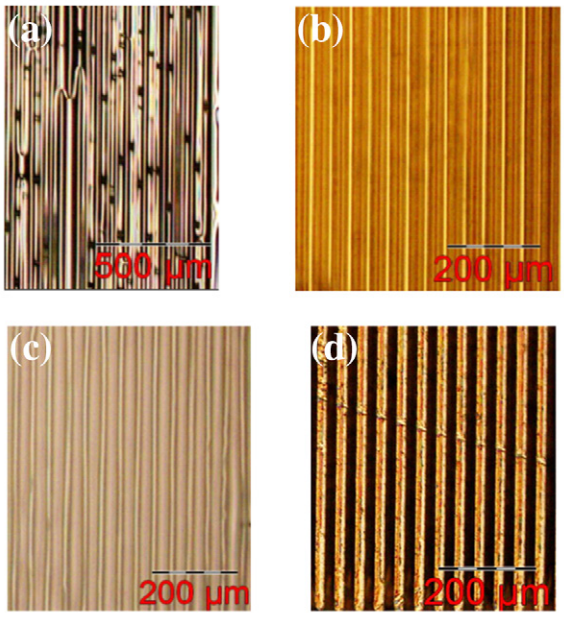

Figure 10. (*a*) Optical microscopic image of the grating fabricated in the polymer film with an initial thickness of 16 μm. The grating stripe emerges partially ruptured in the same line and merging between the adjacent lines, which indicates the unsuccessful replication of the mask. (*b*) Optical microscopic image of the successfully replicated uniform grating in the polymer film with an initial thickness of 23 μm. (*c*) Optical microscopic image of the successfully replicated uniform grating in the polymer film with applied voltage 150 V and an initial thickness 16 μm. The applied voltage in (*a*) and (*b*) is 130 V, the electrode spacing is 45 μm. (*d*) Optical microscopic image of the pre-patterned nickel mask with a grating period of 40 μm, the ridge of the grating has a width of 17 μm and a height of 9 μm.

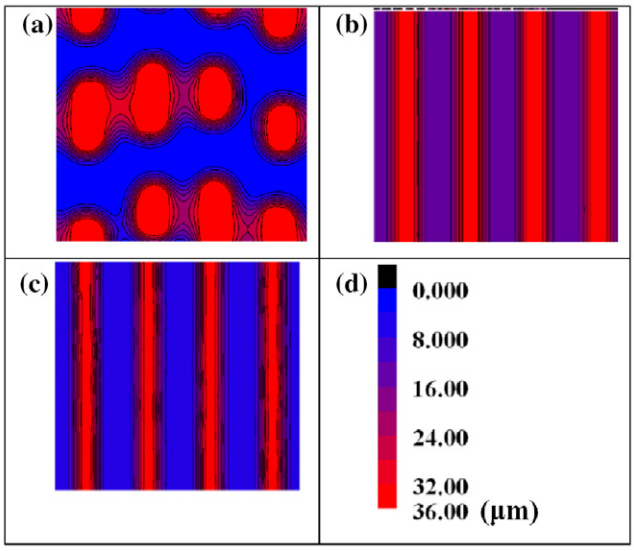

Figure 11. Simulation results corresponding to the experimental results in figure 11. (*a*) The initial film h0 is 16 μm, the applied voltage is 530 V. (*b*) The initial film h0 is 23 μm, the applied voltage is 530 V. (*c*) The initial film h0 is 16 μm, the applied voltage is 600 V. The surface tension γ is 0.038 J m^{-2}, dielectric constant of the film ε1 is 4. (*d*) The surveyor's rod of the simulation results.

film, we compare dimensional time. The dimensional time of evolution for image 6 is t = 14 ms with viscosity 1 Pa.s in figure 2 but t = 1.4 ms with viscosity 0.1 Pa.s in figure 9. Thus, by simply tuning the viscosity of the film, one can effectively control the electrohydrodynamic instability patterning experimental time. In general, the characteristic wavelength is independent of the viscosity ratio between top and bottom fluids as long as they are both perfect insulators, however, the viscosity influences the time for pattern formation strongly. This offers an advantage in EHDIP for decoupling time and length scales by varying the molecular weight of polymers [39].

5. Experimental results

Experiments were conducted to verify the numerical simulation results. The following parameters were taken: a dc voltage of 130 V and 150 V was applied and a hotplate was used to heat the polymer SU8 at the temperature of 120°C for 10 minutes, the electrode space was 45 μm, the period of mask grating is 40 μm, the width and the depth of the grating is 17 μm and 9 μm, respectively. The results of the experiments are shown in the optical micrographs in figure 10. Here, the induced faithful structure has the same period of 40 μm (figures 10(*b*) and 10(*c*)) as that of the mask as shown in figure 10(*d*). Depending on spatiotemporal modulation of the electric field, we observe either a perfect grating pattern with no flaws (figures 10(*b*) and 10(*c*)) or a striped structure where the grating emerges partially ruptured along the same line and merged with a neighboring grating (figure 10(*a*)). The different ordering phenomena originate from the different initial thicknesses h_0 of the polymer film and the varied applied voltages. Figure 10(*a*) shows that faithful replication cannot be realized when the initial thickness h_0 is 16 μm and the applied voltage is 130 V. However, faithful replication can be realized in figure 10(*b*) when the initial

thickness h_0 is 23 μm. In addition, by increasing the applied voltage to 150 V, as shown in figure 10(*c*), grating structures can be obtained in the polymer film.

The simulation results in figure 11 correspond to the experimental results with the process parameters such as the period, width and depth of electrode protrusion, the initial film thickness, electrode spacing being the same for the two sets of figures. The surface tension γ is 0.038 J m^{-2}, dielectric constant of the film ε_1 is 4 in figure 11. A slight deviation between the theoretical and experimental voltage is witnessed, which might be due to the mismatch of surface tension and dielectric constant of the film between the simulation model and experimental study. Ordered and disordered patterns can be clearly seen in figure 11.

6. Conclusions

This article uses a three-dimensional model to simulate the electrostatic field induced thin-film instability process. The simulation results reveal that the replication of the given pattern in the mask can be obtained only when certain conditions are met. It is found that larger initial film thickness and higher applied voltage help to achieve the replication of the pattern. Furthermore, it is found that a higher dielectric constant and smaller surface tension are helpful for achieving replication of the mask with a smaller period. Although decreasing the viscosity of the polymer shortens the duration of the replication process, it does not affect the replication results. For a fixed separating distance between the template and the substrate, if the polymer thickness changes, the air gap varies accordingly, leading to different ΔP values. Increasing the film thickness means decreasing the air gap, which increases the pressure difference ΔP, so we just discuss the effect of film thickness on the pressure difference ΔP. Among the process parameters, consisting of surface tension, voltage, polymer thickness, dielectric constant, the voltage is the most critical factor, by which the experiments can be performed flexibly. In general, these simulation results are helpful for the experimental control in obtaining uniform ordered patterns in polymer with desired feature sizes.

Acknowledgments

The authors acknowledge funding from the Natural Science Foundation of China under grant numbers 90923036 and 60977041. Financial support from the 100 Talents Program of Chinese Academy of Sciences is also acknowledged. The financial support of the UK Innovative electronic Manufacturing Research Centre (IeMRC) is also acknowledged through the funding of the Flagship project "Smart Microsystems" (FS/01/02/10).

References

[1] Chou S Y and Zhuang L 1999 Lithographically induced self-assembly of periodic polymer micropillar arrays *J. Vac. Sci. Technol.* B **17** 3197–202
[2] Chou S Y, Zhuang L and Guo L 1999 Lithographically induced self-construction of polymer microstructures for resistless patterning *Appl. Phys. Lett.* **75** 1004–6
[3] Schäffer E, Thurn-Albrecht T, Russell T P and U Steiner 2000 Electrically induced structure Formation and pattern transfer *Nature.* **403** 874–7
[4] Yang Hin T, Liu C, Conway P P, Yu W, Marc P and Desmulliez Y 2010 Fabrication of a polymeric optical waveguide-on-flex using electrostatic-induced lithography *IEEE Photon. Technol. Lett.* **22** 957–9
[5] Schäffer E, Thurn-Albrecht T, Russell T P and Steiner U 2001 Electrohydrodynamic instabilities in polymer films *Europhys. Lett.* **53** 518
[6] Onuki A 1995 Interface instability induced by an electric field in fluids *Physica* A. **217** 38–52
[7] Tomar G, Shankar V, Sharma A and Biswas G 2007 Electrohydrodynamic instability of a confined viscoelastic liquid film *J. Non-Newtonian Fluid Mech.* **143** 120–30
[8] Tian E M, Svobodny T P and Phillips J D 2011 Thin liquid film morphology driven by electro-static field *Appl. Math. Mech.* **32** 1039–46
[9] El-Sayed M F, Moussa M H M, Hassan A A A and Hafez N M 2011 Electrohydrodynamic instability of two thin viscous leaky dielectric fluid films in a porous medium *Appl. Math.* **2011** 498718
[10] Russell T P, Lin Z, Schäffer E and Steiner U 2003 Aspects of electrohydrodynamic instabilities at polymer interfaces *Fibers and Polymers* **4** 1–7
[11] Sarkar J, Sharma A and Shenoy V B 2008 Electric-field induced instabilities and morphological phase transitions in soft elastic films *Phys. Rev.* E. **77** 031604
[12] Partho S, Pattader G, Banerjee I, Sharma A and Bandyopadhyay D 2011 Multiscale pattern generation in viscoelastic polymer films by spatiotemporal modulation of electric field and control of rheology *Adv. Funct. Mater.* **21** 324–35
[13] Lin Z, Kerle T and Russell T P 2002 Structure formation at the interface of liquid/liquid bilayer in electric field *Macromolecules* **35** 3971–6
[14] Pease L F III and Russel W B 2002 Linear stability analysis of thin leaky dielectric films subjected to electric fields *J. Non-Newtonian Fluid Mech.* **102** 233–50
[15] Pease III L F and Russel W B 2003 Electrostatically induced submicron patterning of thin perfect and leaky dielectric films: A generalized linear stability analysis *J. Chem. Phys.* **118** 3790–803
[16] Hun Lee S, Kim P, Eui Jeong H and Suh K Y 2006 Electrically induced formation of uncapped, hollow polymeric microstructures *J. Micromech. Microeng.* **16** 2292
[17] Arun N, Sharma A, Partho S, Pattader G, Banerjee I, Dixit H M and Narayan K S 2009 Electric-field-induced patterns in soft viscoelastic films: from long waves of viscous liquids to short waves of elastic solids *Phys. Rev. Lett.* **102** 254502
[18] Lyutakov O, Tuma J, Prajzler V, Huttel I, Hnatowicz V and Švorčík V 2010 Preparation of rib channel waveguides on polymer in electric field *Thin Solid Films* **519** 1452–7
[19] Deshpande P, Sun X and Chou S Y 2001 Observation of dynamic behavior of lithographically induced self-assembly of supramolecular periodic pillar arrays in a homopolymer film *App. Phys. Lett.* **79** 1688–90
[20] Li X, Shao J, Ding Y, Tian H and Liu H 2011 Improving the height of replication in EHD patterning by optimizing the electrical properties of the template *J. Micromech. Microeng.* **21** 115004
[21] Morariu M,Voicu N, Schäffer E, Lin Z, Thurn-Albrecht T, Russell T P and Steiner U 2003 Hierarchical structure formation and pattern replication induced by an electric field *Nat. Mater.* **2** 48–52
[22] Ning W and Russel W B 2005 Dynamics of the formation of polymeric microstructures induced by electrohydrodynamic instability *App. Phys. Lett.* **86** 241912

[23] Pease III L F and Russel W B 2006 Charge driven, electrohydrodynamic patterning of thin films *J. Chem. Phys*. **125** 184716
[24] Mondal K, Kumar P and Bandyopadhyay D 2013 Electric field induced instabilities of thin leaky bilayers: Pathways to unique morphologies and miniaturization *J. Chem. Phys.* **138** 024705
[25] Kim D and Lu W 2006 Interface instability and nanostructure patterning *Comput. Mater. Sci*. **38** 418–25
[26] Verma R, Sharma A, Kargupta K and Bhaumik J 2005 Electric field induced instability and pattern formation in thin liquid films *Langmuir* **21** 3710–21
[27] Bandyopadhyay D, Sharma A, Thiele U and Dinesh Sankar Reddy P 2009 Electric-field-induced interfacial instabilities and morphologies of thin viscous and elastic bilayers *Langmuir* **25** 9108–18
[28] Atta A, Crawford D G, Koch C R and Bhattacharjee S 2011 Influence of electrostatic and chemical heterogeneity on the electric-field-induced destabilization of thin liquid films *Langmuir* **27** 12472–85
[29] Ning W and Russel W B2006 Electrohydrodynamic instability of dielectric bilayers: kinetics and thermodynamics *Ind. Eng. Chem. Res.* **45** 5455–65
[30] Samanvaya Srivastava P, Sankar Reddy D,Wang C, Bandyopadhyay D and Sharma A 2010 Electric field induced microstructures in thin films on physicochemically heterogeneous and patterned substrates *J. Chem. Phys.* **132** 174703
[31] Ning W, Pease III L F and Russel W B 2005 Electric-field-induced patterns in thin polymer films: weekly nonlinear and fully nonlinear evolusion *Langmuir* **21** 12290–302
[32] Ning W and Russel W B 2009 Micro- and nano-patterns created via electrohydro-dynamic instabilities *Nano Today* **4** 180–92
[33] Li H *et al* 2013 Simulation and modelling of sub-30 nm polymeric channels fabricated by electrostatic induced lithography *RSC Adv.* **3** 11839–45
[34] Tian H, Shao J, Ding Y, Li X and Liu H 2013 Numerical characterization of electrohydrodynamic micro- or nanopatterning processes based on a phase-field formulation of liquid dielectrophoresis *Langmuir* **29** 4703–14
[35] Heier J, Groenewold J and Steiner U 2009 Pattern formation in thin polymer films by spatially modulated electric fields *Soft Matter* **5** 3997–4005
[36] Harkema S 2005 Capillary instabilities in thin polymer films mechanism of structure formation and pattern replication *Phd Thesis* University of Groningen, The Netherlands
[37] Ning W 2008 Nonliner dynamics of pattern formation via electrohydrodynamic instabilities *Phd Thesis* Princeton University, NJ, USA
[38] Lin Z, Kerle T, Russell T P, Schaffer E and Steiner U 2002 Electric field induced dewetting at polymer/polymer interfaces *Macromolecules* **35** 6255–62
[39] Lin Z, Kerle T, Baker S M, Hoagland D A, Schaffer E, Steiner U and Russell T P 2001 Electric field induced instabilities at liquid/liquid interfaces *J. Chem. Phys.* **114** 2377–81
[40] Theodossiou G, Nelson J K and Odell G M 1986 A computer simulation of transient electrohydro-dynamic motion in stressed dielectric liquids *J. Phys. D: Appl. Phys.* **19** 1643–56